



RESEARCH ARTICLE

Regulation of Pro-Apoptotic Bax and Trail Gene Expressions by H5N1 in Madin-Darby Canine Kidney (Mdck) Cell Line

Wei Boon Yap^{1,2*}, Kah Chun Goh¹, Sharifah Syed Hassan³ and Vinod RMT Balasubramaniam³

¹Biomedical Science Programme, Faculty of Health Sciences, Universiti Kebangsaan Malaysia, Jalan Raja Muda Abdul Aziz, 50300 Kuala Lumpur, Malaysia; ²Center of Toxicology and Health Risk Studies, Faculty of Health Sciences, Universiti Kebangsaan Malaysia, Jalan Raja Muda Abdul Aziz, 50300 Kuala Lumpur, Malaysia; ³Jeffrey Cheah School of Medicine & Health Sciences, Monash University Malaysia, Jalan Lagoon Selatan, 46150 Bandar Sunway, Selangor, Malaysia

*Corresponding author: yapweiboon@ukm.edu.my

ARTICLE HISTORY (20-149)

Received: March 30, 2020
Revised: May 29, 2020
Accepted: June 02, 2020
Published online: June 18, 2020

Key words:

Bax
Cellular apoptosis
DNA fragmentation
H5N1
Influenza
TRAIL

ABSTRACT

Avian influenza virus (AIV) A H5N1 is able to cause zoonosis with high morbidity and mortality. Several studies suggested the regulation of cellular apoptosis for virus survival by influenza viruses. This sheds light on the development of antivirals that can improve cellular apoptosis to fight influenza infections. This study aimed to investigate the regulation of pro-apoptotic gene expressions by H5N1 in MDCK cells. The H5N1 infection ($10^{2.67}$ TCID₅₀/ml) was performed for 8, 24, 48, 72, 96 and 120 hours. Upon incubation, the percentage of cell death, DNA fragmentation and pro-apoptotic gene expressions i.e. *Bax*, *TRAIL*, *Caspase 3* (*Cas3*) and *8* (*Cas8*), and *Fas-ligand* (*FasL*) were determined. The degree of DNA laddering and pro-apoptotic gene expressions were determined on agarose gels. The results indicated that severe cytopathic effects (CPE) caused by H5N1 appeared as early as 24 hour post-infection (hpi) meanwhile a significant cell death was observed starting at 48 hpi. However, DNA laddering was not observed in both of the control and infected DNA samples. Downregulation of *Bax* gene expression was recorded at 24-72 hpi and a total suppression was observed at 96 and 120 hpi. Similarly, a significant decrease in the *TRAIL* gene expression was observed at 48-120 hpi. On the contrary, the expressions of *Cas3*, *Cas8* and *FasL* genes were not detected in the mock and infected samples. Conclusively, this study suggested that H5N1 might downregulate cellular apoptosis prematurely for viral survival which can be a target cellular mechanism for newly developed antivirals to combat H5N1 infections.

©2020 PVJ. All rights reserved

To Cite This Article: Yap WB, Goh KC, Hassan SS, Balasubramaniam VRMT 2020. Regulation of pro-apoptotic bax and trail gene expressions by H5N1 in madin-darby canine kidney (Mdck) cell line. Pak Vet J, 40(4): 509-513. <http://dx.doi.org/10.29261/pakvetj/2020.055>

INTRODUCTION

Avian influenza A virus (AIV) H5N1, also known as bird flu virus, is a zoonotic viral pathogen that can be transmitted to human through close contact with infected animals, predominantly avian species such as ducks, geese and chicken (Yap *et al.*, 2018). AIV H5N1 can cause mortality more than 50% if spilled over to human hosts. In 2003 to 2019, the cumulative number of confirmed H5N1 cases was 861 including 455 deaths (Yap *et al.*, 2018).

The current influenza antivirals inhibit predominantly the viral surface antigens such as the neuraminidase (NA) and matrix (M) proteins in order to block the viral infections and replication cycle (Yap *et al.*, 2018).

However, resistance to antivirals has been reported. For instance, the M2 protein inhibitors such as amantadine and rimantadine that are no longer recommended by the Centers for Disease Control and Prevention (CDC). Likewise, there is evidence of viral resistance to neuraminidase inhibitors such as oseltamivir, zanamivir and peramivir that prevent viral release from host cells. As a result, the search of alternative therapeutics that help enhance cellular responses instead of those targeting viral surface proteins has been proposed (Lina *et al.*, 2018; Mehdbod *et al.*, 2019).

Cellular apoptosis is involved in both of the induction of anti-influenza immune responses and the enhancement of the pathogenicity of H5N1 (Uprasertkul *et al.*, 2007;

Mehdbod *et al.*, 2019). During influenza virus infections, host cells scavenge the viral antigens, e.g. nucleocapsid (NP), nonstructural 1 (NS1) and PB1-F2 proteins and get sensitized. This initiates the intrinsic apoptotic pathway via the activation of cell death agonists, such as Bax that forms pores on the mitochondrial membrane and destabilizes it (Lee *et al.*, 2019). The extrinsic apoptotic pathway is, on the other hand, activated via interactions of death receptors with their counterparts, for instance the Fas ligand (FasL) and tumour necrosis factor (TNF)-related apoptosis-inducing ligand (TRAIL) following influenza virus infections. Altogether, the activation of intrinsic and extrinsic pathways trigger cellular apoptosis via a cascade of caspase activities [e.g. caspase 8 (Cas8), 9 (Cas9) and 3 (Cas3)] in order to contain the virus infections (Zhang *et al.*, 2020). Several studies reported that the upregulated expressions of *Bax* (Bulanova *et al.*, 2017) and *TRAIL* (Ishikawa *et al.*, 2005; Brincks *et al.*, 2008) genes sensitized virally infected host cells to undergo premature apoptosis hence termination of H5N1 infections. However, Pizzorno *et al.* (2018) documented the contrary observation in which a few influenza virus strains blocked the occurrence of apoptosis prematurely in order to ensure virus replication. In view of this, the regulation of cellular apoptosis by influenza viruses is somewhat strain-dependent. It is, therefore, very important to better apprehend the regulation of cellular apoptosis by individual influenza viruses especially those posing great threats to human health like AIV H5N1.

In Malaysia, AIV H5N1 has caused occasional outbreaks in the poultry industry in Malaysia (Yap *et al.*, 2018), hence its impacts on human health should not be neglected. This study aimed to investigate the manipulation of cellular apoptosis by H5N1 in infected MDCK cells. The results implied that the virus inhibited the expression of *Bax* and *TRAIL* genes prematurely. This provides quintessential information to the development of antivirals that can help improve the cellular apoptosis in order to halt H5N1 infections.

MATERIALS AND METHODS

Propagation of AIV H5N1 and determination of viral titer: MDCK cell line (ATCC, USA) was grown in RPMI 1640 (Gibco, Germany) containing 10% (v/v) FBS and 1% (v/v) Pen-Strep (10,000 U/mL Penicillin, 10,000 µg/mL Streptomycin) at 37°C with 5% CO₂. The AIV H5N1 (A/chicken/5858/2004/Malaysia) was propagated in 80% confluent MDCK cells. The experiments were performed in a biosafety level two-plus (BSL-2+) setting with sufficient personal protective equipments (PPEs) such as face masks and shields, gloves and disinfection with 70% (v/v) ethanol before and after experimentations. The experimental waste was decontaminated with autoclave before disposal.

To determine the viral titer, serial dilutions of virus (10^2 - 10^{10}) were used to infect MDCK cells on 24-well plates. Four wells of cells were infected with each virus dilution. Uninfected cells were prepared as control. The virus adsorption was allowed for 2 h, the medium was replaced and the cells were further incubated for 48 h. The cytopathic effects (CPEs) were observed and the virus titer was expressed as 50% tissue culture infectious dose (TCID₅₀) in which cells in two of the four wells showed CPEs.

Percentage of cell death: MDCK cells were infected with H5N1 at TCID₅₀ in quadruplicate for 8, 24, 48, 72, 96 and 120 h. Uninfected cells were prepared as negative control. At each designated time point, the cells were collected, stained with 0.4% (w/v) trypan blue and the viable/dead cells were enumerated with a hemocytometer.

Extraction of DNA and total RNA: The cells were collected at the designated time points as described previously and lysed with Trizol LS (Invitrogen, USA). The lysate was mixed with 200 µL of chloroform, vortexed and incubated in room conditions for 15 min. The mixture was then centrifuged (12,000 xg, 4°C) to collect the upper layer (total RNA) and the interphase (DNA).

The upper layer was mixed with 500 µL of isopropanol and incubated in room conditions for 10 min. The RNA was pelleted (12,000 xg, 4°C for 10 min) and then rinsed with 1 mL of 75% (v/v) ethanol. The RNA pellet was air-dried and then dissolved in 20 µL of nuclease-free water.

About 300 µL of absolute ethanol was added into the interphase. The mixture was incubated in room conditions for 3 min and then spun (2000 xg, 4°C) for 5 min. The DNA pellet was first resuspended in 1 mL of 0.1 M sodium citrate (pH 8.5), spun down and dissolved in 75% (v/v) ethanol. The DNA pellet was again retrieved by centrifugation, air-dried and reconstituted in 8 mM NaOH. The pH was adjusted to 7-8 with 0.1 M HEPES.

DNA fragmentation: The DNA fragmentation analysis was carried out as demonstrated by Dharmayanti *et al.* (2017). The DNA concentration was adjusted to 27.1 ng/µL and then mixed with 6X Run Safe Dye (Cleaver Scientific Ltd, UK). The samples were electrophoresed on a 1.5% (w/v) agarose gel at 80 V for 1 h.

Reverse transcription and polymerase chain reaction: The first-strand cDNA was generated using the total RNA (396 ng), oligo-dT random primers (500 ng) and the M-MLV reverse transcriptase (Promega Inc., USA) at 37°C for 1 h. The H5N1 *NS1*, *GADPH*, *Bax*, *TRAIL*, *Cas3*, *Cas8* and *FasL* genes were amplified from the cDNA using the primer pairs in Table 1. The amplification mixture contained EconoTaq PLUS Green 2X Master Mix (Lucigen, USA), 2.5 µL of cDNA and 1 µM of forward and reverse primers. The PCR cycling conditions were as follows: initial denaturation at 94°C for 120 s, 35 cycles of 94°C for 30 s, 55°C for 30 s, 72°C for 1 min, and final extension at 72°C for 10 min. The PCR products were electrophoresed on a 1.5% (w/v) agarose gel at 80 V for 1 h and then analysed using ImageJ (<https://imagej.nih.gov/ij>). The expressions of the target apoptotic genes were normalized with that of the *GADPH* gene and expressed as relative expression levels (%).

RESULTS

Percentage of cell death: MDCK cells were infected with H5N1 at $10^{2.67}$ TCID₅₀/mL. As shown in Fig. 1, CPE started to appear as early as 24 h post-infection (hpi) [Fig. 1(b)] in which infected cells became rounded, elongated with cellular projections and nuclear condensation compared to those observed at 8 hpi [Fig. 1(a)]. The CPE was further exacerbated at 48 hpi [Fig. 1(c)] when a

substantial number of dead cells detached from the bottom of the flask. The cell death became more plausible at 72 hpi [Fig. 1(d)] and almost all dead cells detached from the bottom of the flask at 96 [Fig. 1(e)] and 120 [Fig. 1(f)] hpi.

In spite of the CPEs appearing as early as 24 hpi, a significant cell death (31.77%) was only recorded starting at 48 hpi (Fig. 2). The cell death increased drastically and rapidly at 72 hpi (50.15%) and spiked at 96 (94.15%) and 120 hpi (98.14%). For the uninfected or control MDCK cells, the percentage of cell death increased at a very much slower rate throughout the incubation period and only reached 56.75% after 120 hours of incubation.

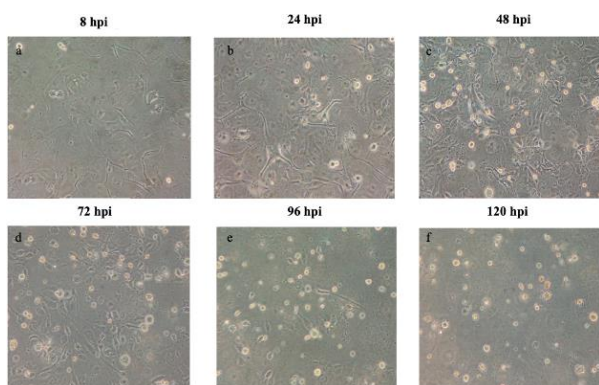


Fig. 1: CPEs caused by H5N1 in MDCK cells at 8, 24, 48, 72, 96 and 120 hpi under an inverted light microscope at 20X magnification. The severity of H5N1 infection increased progressively over the incubation period.

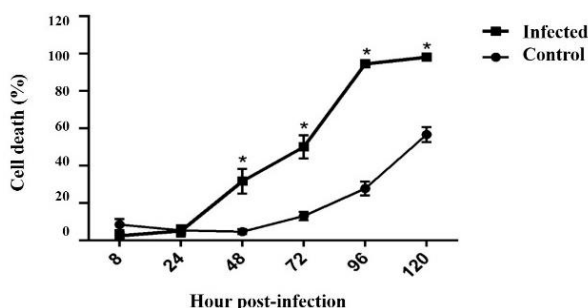


Fig. 2: Percentage of death of the control and H5N1-infected MDCK cells. The cell death increased progressively with the infection period. The data are presented as mean value \pm SEM (n=4). *indicates statistically significant with $P < 0.05$.

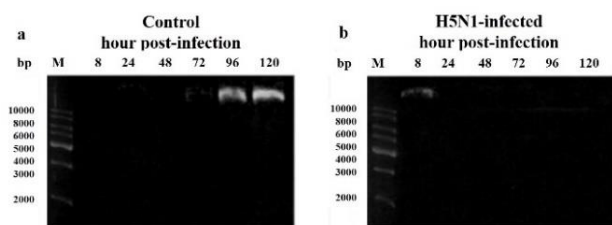


Fig. 3: DNA fragmentation analysis in the (a) control and (b) H5N1-infected MDCK cells. The cellular DNA larger than 10 kbp was observed in (a) at 96 and 120 hpi, and (b) at 8 hpi.

DNA fragmentation: In this study, the regulation of cellular apoptosis by AIV H5N1 in MDCK cells was first investigated by examining the degree of DNA fragmentation on an agarose gel. In apoptosis, the nuclear DNA is degraded by the caspase-activated DNase (CAD) into smaller pieces hence the DNA laddering. As shown in Fig. 3(a) and (b), DNA bands larger than 10 kb appeared on the lanes for the control samples collected at 72-120 hpi, whereas the cellular DNA was only present on the lane for the infected sample collected at 8 hpi. There was absence of DNA laddering in both of the infected and control samples collected at 8 to 120 hpi. Collectively, this is likely to imply an early inhibition of apoptosis by AIV H5N1 in MDCK cells.

Expression of pro-apoptotic genes in H5N1-infected MDCK cells: The AIV H5N1 infection in MDCK cells was first authenticated with the presence of *NS1* gene [Fig. 4(a)]. The *NS1* gene was not detected in the control samples but was consistently and constantly amplified from the infected samples. Amongst the target apoptotic genes, the *Cas3* (849 bp) and *Cas8* (387 bp) genes were unsuccessfully amplified from both of the control and H5N1-infected samples [Fig. 4(a)]. Meanwhile, the *FasL* (342 bp) gene amplification produced multiple unspecific amplicons [Fig. 4(a)].

In terms of the *Bax* and *TRAIL* gene expressions, their expressions remained unchanged throughout the incubation period (8-120 hpi) in the control samples. However, in the presence of H5N1 infection, there was a significant downregulation (~40%) of *Bax* gene expression starting at 24 hpi [Fig. 4(a) and (b)]. Surprisingly, the reduction was observed even earlier than the H5N1-induced cell death (48 hpi). A downregulation greater than 50% continued at 48 and 72 hpi [Fig. 4(b)], and the *Bax* gene expression was completely undetectable at 96 and 120 hpi. The findings support our earlier speculation that the rapidly replicating H5N1 virus might overcome cellular apoptosis prematurely via the downregulation *Bax* gene in susceptible MDCK cells.

The expression of *TRAIL* gene, on the other hand, was downregulated slightly later than that of the *Bax* gene. A significant downregulation of *TRAIL* gene was recorded at 48 and 72 hpi [Fig. 4(a)]. The reduction was greater than 50% at both time points [Fig. 4(c)]. Collectively, the downregulation of pro-apoptotic *Bax* and *TRAIL* gene expressions as early as 24 and 48 hpi, respectively indicates an arrest of early cellular apoptosis and also explains the absence of DNA fragmentation observed earlier in this study. The early inhibition of cellular apoptosis by AIV H5N1 also suggests that apoptosis or programmed cell death may not be the main cause of death for infected cells.

Table 1: Primers used in the gene amplification

Gene	Forward primer sequence (5'-3')	Reverse primer sequence (5'-3')
<i>Bax</i>	TTCATGGACGGGTCCGGGGAG	TTATCAGCCCATCTTCTTCCAGATG
<i>TRAIL</i>	ACCATTTCTACAGTTCCAGAAA	TCCTGAAAT CGAAAGTATGTTT
<i>Cas3</i>	TTAATAAAGGTATCCATGGAGAACA	TTAGTGATAAAAATAGAGTTCTTTTGTGAG
<i>Cas8</i>	GATATTGGGGAACAACCTGGAC	CATGTCATCATCCAGTTTGCA
<i>FasL</i>	GATTGGGCCTGGGGATGTTTCA	TGTGGCTCAGGGGCAGGTTGTTG
<i>NS1</i>	AAGGATCATAGCTCGAGAGATTCCAACACTGTG	GCAGTTTTCGAATTCACCTTCTGACTCAAT
<i>GAPDH</i>	AAGGTGAAGGTCGGAGTCAAC	GGGGTCAAT GATGGCAACAATA

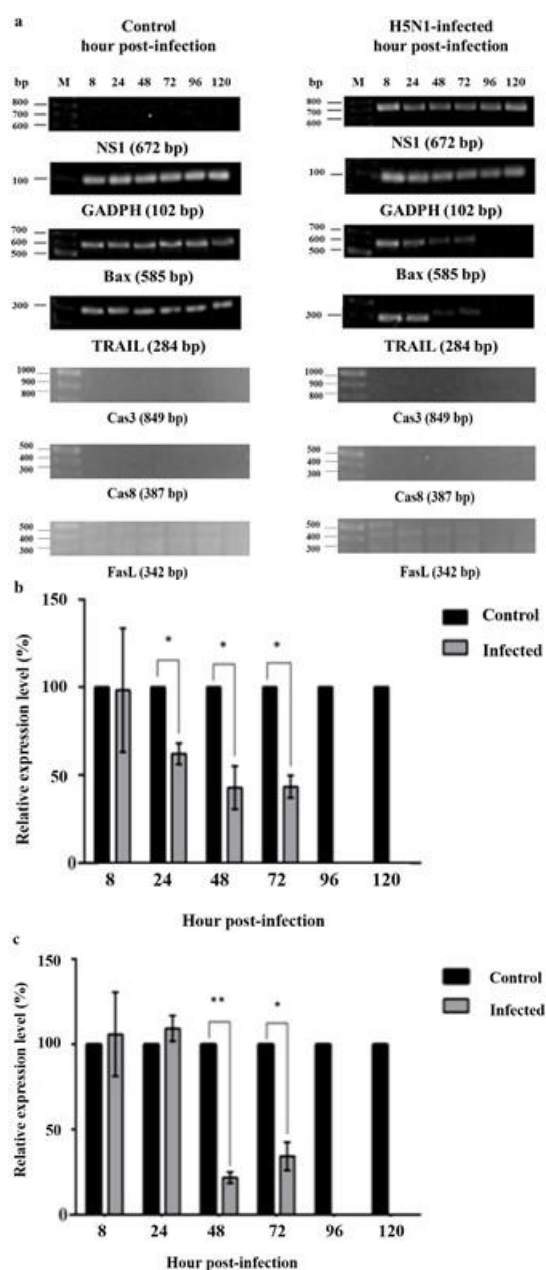


Fig. 4: *Bax* and *TRAIL* gene expressions in the control and H5N1-infected MDCK cells. (a) The gene expression analysis of H5N1 *NS1*, *GAPDH*, *Bax*, *TRAIL*, *Cas3*, *Cas8* and *FasL* using agarose gel electrophoresis. The relative expression levels of (b) *Bax* and (c) *TRAIL* genes in H5N1-infected MDCK cells compared with that of the internal control (*GAPDH*). The data are presented as mean value \pm SEM ($n=2$). *indicates statistically significant with $P<0.05$, while **indicates $P<0.01$.

DISCUSSION

Programmed cell death or apoptosis has been viewed as an important cellular innate immunity to block the replication of invading pathogens such as viruses (Jorgensen *et al.*, 2017). Uprasertkul *et al.* (2007) demonstrated that AIV H5N1 infection triggered cellular apoptosis which was responsible for the destruction of alveolar epithelial cells and pneumonia. In this study, a similar phenomenon was observed. An inclining death rate of AIV H5N1-infected cells was recorded along with the gradual appearance of CPEs. The appearance of CPEs was noted with a few signature morphological changes of infected cells such as rounded, elongated with cellular projections and nuclear condensation (Zhang *et al.*, 2020).

This is in line with that reported by Tan *et al.* (2016a). On the other hand, the relatively slower death rate seen in the uninfected MDCK cells was mainly due to cell senescence and depletion of nutrients in the medium over time (Tan *et al.*, 2016b).

Principally, during cellular apoptosis, the CAD cleaves the cellular DNA into oligonucleosomal fragments that form a laddering pattern when resolved using agarose gel electrophoresis (Zhang *et al.*, 2020). However, in this study, the DNA laddering was not observed and it is suggested to be attributable to an early arrest of apoptosis by H5N1 infection in MDCK cells. The finding was similar with that reported by Dharmayanti *et al.* (2017) in which there were no signs of DNA fragmentation in infected cells following infections by three Indonesian H5N1 isolates. It is speculated that instead of apoptosis, necrosis might play a more significant role in H5N1-induced cell death due to the rapid virus replication in highly susceptible host cells like MDCK (Tan *et al.*, 2016a; Lee *et al.*, 2019). Furthermore, Kurokawa *et al.* (1999) reported that rapidly replicating viruses like H5N1 prevent cellular apoptosis so that they can evade the host innate immune responses to ensure its survival.

In the DNA fragmentation analysis, the overall quality of genomic DNA extracted from both of the control and infected cells using the Trizol reagent was less satisfactory. It is reported that loss of DNA at the interphase layer is commonly observed in DNA extraction and precipitation using organic solvents like Trizol and ethanol (Jakubowska *et al.*, 2012).

As discussed earlier, the rapidly replicating H5N1 virus is speculated to prevent premature apoptosis in order to perpetuate its replication in host cells. In order to better understand how H5N1 overcomes apoptosis for its replication, the expressions of pro-apoptotic genes were examined. Cellular apoptosis occurs through two major mechanisms, namely (i) the intrinsic pathway via destabilization of mitochondrial membrane by pro-apoptotic proteins such as Bax (Leong *et al.*, 2016; Basri *et al.*, 2018) and (ii) the extrinsic pathway that implicates interactions of pro-apoptotic ligands such as TRAIL and FasL with their death receptors on cell surfaces (Zhou *et al.*, 2017). The activation of intrinsic and extrinsic pathways, in turn, promotes the synthesis of initiator (e.g. Cas8) and executor (Cas3) caspases to induce programmed cell death (Mehrbod *et al.*, 2019). In this study, the expressions of *Bax* and *TRAIL* genes were found to be downregulated progressively. In order to rule out the effect of cell death (starting at 48 hpi) on the *Bax* and *TRAIL* gene downregulations, an internal control gene, *GAPDH* was included. The unchanged expression of *GAPDH* gene in infected MDCK cells throughout the incubation period indicated that the downregulation of *Bax* and *TRAIL* gene expressions was mostly a result of AIV H5N1 infection. The downregulation is possibly a counteraction of AIV H5N1 to prevent the initiation of cellular apoptosis that eventually undermines the virus replication (Kurokawa *et al.*, 1999). This is well corroborated by Bulanova *et al.* (2017) that showed the activation of cellular apoptosis via upregulation of BCL-2 proteins such as Bax limited the replication of influenza viruses. In addition, a similar observation was also reported by Xing *et al.* (2009) in which the expression of

TRAIL gene was downregulated by 4.2 folds in avian macrophages infected with AIV H9N2. The suppression of *TRAIL* on the infected cell surfaces reduces cytotoxic T cell responses that are responsible for the clearance of virally infected cells (Brincks *et al.*, 2008).

In spite of the progressive downregulation of *Bax* and *TRAIL* gene expressions observed in this study, it is noteworthy that the regulation of apoptosis by influenza viruses is strain-dependent. For instance, AIV H5 subtype upregulates the expression of *TRAIL* *in vitro* and *in vivo* (Cherdantseva *et al.*, 2019), whereas the H9 subtype significantly suppresses the expression of *TRAIL* in chicken macrophages (Xing *et al.*, 2009). It is, therefore, indispensable to study the regulation of cellular apoptosis by individual influenza viruses as it may provide useful information for the development of anti-influenza that targets the apoptotic pathway to fight influenza virus infections.

Besides the *Bax* and *TRAIL* gene expressions, the effects of H5N1 infection on the *Cas3*, *Cas8* and *FasL* gene expressions were also investigated in this study. However, the target genes were not amplified from the control and infected samples. It is highly recommended that optimizations of primers and amplification conditions in prospective studies might provide a more comprehensive observation corresponding to the regulation of *Cas3*, *Cas8* and *FasL* gene expressions by the H5N1 infection. Zheng *et al.* (2019) demonstrated that the specificity and sensitivity of gene amplification could be vastly improved by optimizing the amplification parameters, for instance, the primer and MgCl₂ concentrations, number of amplification cycles and annealing temperature.

Although the results suggested that the H5N1 infection arrested cellular apoptosis prematurely via the inhibition of *Bax* and *TRAIL* gene expressions in MDCK cells, several limitations have been recognized in this study, among others, the breadth of the inhibitory actions can be further elucidated via advanced molecular techniques such as quantitative real-time PCR (qRT-PCR) and Western blotting (WB). Even though the execution of qRT-PCR is more costly and the analysis requires highly trained personnel, it allows monitoring of the amplification processes and quantification of the template amount concomitantly, hence a more accurate measurement of the target gene expression (Tan *et al.*, 2016b). The expressions of apoptotic gene products, on the other hand, can be determined using the WB. The WB results can provide a more deliberate explanation on how the regulation of apoptotic gene expressions by H5N1 affects the functions of the gene products and the cellular apoptotic events (Lee *et al.*, 2019).

Conclusions: In general, programmed cell death or apoptosis is a cellular innate immune response to stop virus replication. This study showed that the cellular apoptosis might not be the main reason for H5N1-induced cell death. This observation was supported by (i) the absence of DNA fragmentation with an increase in the cell death percentage; (ii) downregulation of pro-apoptotic *Bax* and *TRAIL* gene expressions prematurely. The suppression of *Bax* and *TRAIL* gene expressions by AIV H5N1 is believed to prevent premature apoptosis and evade cellular immunity; this, in turn, promotes the virus replication. Conclusively, this study is important for the development of anti-influenza agents that can promote cellular apoptosis to block influenza virus infections.

Acknowledgements: This work was supported by the Fundamental Research Grant Scheme (FRGS) by the Malaysia Ministry of Education (FRGS/1/2017/STG05/UKM/02/9).

Authors contribution: All authors discussed and designed the flow of the study. WBY and KCG executed the experiments, collected, analysed and interpreted the data. WBY prepared the manuscript and all authors critically revised the contents of the write-up and approved the submitted version of the manuscript.

REFERENCES

- Basri DF and Subramaniam S, 2018. Effect of *Canarium odontophyllum* stem bark extract against human colorectal cancer cell line HCT 116. *Int J Med Res Pharma Sci* 5:10-8.
- Brincks EL, Katewa A, Kucaba TA, *et al.*, 2008. CD8 T cells utilize *TRAIL* to control influenza virus infection. *J Immunol* 181:4918-25.
- Bulanova D, lanevski A, Bugai A, *et al.*, 2017. Antiviral properties of chemical inhibitors of cellular anti-apoptotic Bcl-2 proteins. *Viruses* 9:271.
- Cherdantseva L, Kovner A, Sharkova T, *et al.*, 2019. Death mechanisms of pulmonary alveolocytes in mice infected with influenza viruses A/H1N1/California/04/2009 and A/H5N1/Goose/Krasnoozers koye/627/05. *Bull Exp Biol Med* 166:637-40.
- Dharmayanti NI, Ukhti DR, Syamsiah F, *et al.*, 2017. Apoptosis study of Indonesian avian influenza virus subtype H5N1 in Madin-Darby Canine Kidney cells. *J Ked Hewan* 11:39-44.
- Ishikawa E, Nakazawa M, Yoshinari M, *et al.*, 2005. Role of tumor necrosis factor-related apoptosis-inducing ligand in immune response to influenza virus infection in mice. *J Virol* 79:7658-63.
- Jakubowska J, Maciejewska A and Pawłowski R, 2012. Comparison of three methods of DNA extraction from human bones with different degrees of degradation. *Int J Legal Med* 126:173-8.
- Jorgensen I, Rayamajhi M and Miao EA, 2017. Programmed cell death as a defence against infection. *Cell Death Immunol* 17:151-64.
- Kurokawa M, Koyama A, Yasuoka S, *et al.*, 1999. Influenza virus overcomes apoptosis by rapid multiplication. *Int J Mol Med* 3:527-57.
- Lee ACY, Zhang AJX, Chu H, *et al.*, 2019. H7N9 influenza A virus activation of necroptosis in human monocytes links innate and adaptive immune responses. *Cell Death Dis* 10:442.
- Leong LM, Chan KM, Hamid A, *et al.*, 2016. Herbal formulation C168 attenuates proliferation and induces apoptosis in HCT-116 human colorectal carcinoma cells: role of oxidative stress and DNA damage. *Evid-based Compl Alt Med* doi: 10.1155/2016/2091085.
- Lina B, Boucher C, Osterhaus A, *et al.*, 2018. Five years of monitoring for the emergence of oseltamivir resistance in patients with influenza A infections in the influenza resistance information study. *Influenza Other Resp* 12:267-78.
- Mehrbod P, Ande SR, Alizadeh J, *et al.*, 2019. The roles of apoptosis, autophagy and unfolded protein response in arbovirus, influenza virus, and HIV infections. *Virulence* 10:376-413.
- Pizzorno A, Dubois J, Machado D, *et al.*, 2018. Influenza A viruses alter the stability and antiviral contribution of host E3-ubiquitin ligase Mdm2 during the time-course of infection. *Sci Rep* 8:3746.
- Tan TS, Sharifah SH and Yap WB, 2016a. Significant replication time-points of avian influenza A virus strain H5N1 in madin-darby canine kidney cells. *Malays J Health Sci* 14:17-21.
- Tan TS, Sharifah SH and Yap WB, 2016b. Replication of a Malaysian strain avian influenza A virus H5N1 in madin-darby canine kidney and african green monkey kidney cells. *Sains Malays* 45:787-93.
- Uiprasertkul M, Kitphati R, Puthavathana P, *et al.*, 2007. Apoptosis and pathogenesis of avian influenza A (H5N1) virus in humans. *Emerg Infect Dis* 13:708-12.
- Xing Z, Cardona CJ, Adams S, *et al.*, 2009. Differential regulation of antiviral and proinflammatory cytokines and suppression of Fas-mediated apoptosis by NS1 of H9N2 avian influenza virus in chicken macrophages. *J Gen Virol* 90:1109-18.
- Yap WB, Tan TS and Sharifah SH, 2018. Universal oral vaccine for influenza infections. *Malays J Health Sci* 16:51-64.
- Zhang J, Han Y, Shi H, *et al.*, 2020. Swine acute diarrhoea syndrome coronavirus-induced apoptosis is caspase- and cyclophilin D-dependent. *Emerg Microbes Infect* 9:439-56.
- Zheng Y, Lu B, Yang Y, *et al.* 2019. Rapid identification of medicinal leech by species-specific polymerase chain reaction technology. *Phcog Mag* 15:410-5.
- Zhou X, Jiang W, Liu Z, *et al.*, 2017. Virus infection and death receptor-mediated apoptosis. *Viruses* 9:316-35.